Machine Learning for Warpage Prediction of Fused Deposition Modelling Processed Parts

Davide Nardi (d.nardi@tudelft.nl)
TU Delft: Technische Universiteit Delft

Research Article

Keywords: Classification, Regression, Additive Manufacturing, First-time-right manufacturing

Posted Date: June 1st, 2021

DOI: https://doi.org/10.21203/rs.3.rs-507209/v1

Abstract

This paper provides a methodology for the application of a machine learning-based framework for fused deposition modelling manufacturing. The approach was developed to take into account the influence of the material, the part geometry, the process parameters on the maximum part warpage defined by the user. The results showed the effectiveness of machine learning for both classification and regression purposes so that the printability of the part is firstly provided, based on the selected warpage threshold, and secondly, the part warpage can be predicted within the problem design space variables, i.e. part material, part height, part length, and layer thickness. The limitations of the use of the analytic equation as a data-points generator are widely discussed, along with the future research based on the obtained preliminary results. In conclusion, the described methodology represents a concrete step towards a first-time-right strategy in the field of manufacturing processes.

1 Introduction

Providing a first-time-right manufacturing capability represents a crucial need for current manufacturing processes in which the common trial-and-error approach leads to material waste, poor part reproducibility, high cost, and delay in part certification.

Fused Deposition Modeling (FDM) is the extensively adopted methodology for additive manufacturing (AM) of prototypes, tools, and low-volume products. The technique is based on printers that use a thermoplastic polymer filament which is initially heated up to its melting temperature and then extruded in a layer by layer fashion obtaining a three-dimensional structure [1]. The process reliability in providing high-quality components is still a challenging task due to the lack of complete understanding of the impact of process-related parameters on the manufactured part characteristics and the process productivity [2-14]. This, in turn, prevents the possibility of generalising trends from these results, which were mostly evaluated using Taguchi method and ANOVA analysis.

Machine learning (ML)-based algorithms are permeating several scientific disciplines due to their ability to explore complex pattern in collected data and perform data-driven predictions on new data [15].

ML has been effectively used in FDM applications, addressing the modelling of shape deviations in FDM parts [15], developing real-time detection methods to locate areas of interest in fused filament fabricated layers [16], predicting deposition angles [17], indicating adjustments on 3D models to reduce the dimensional deviations of the printed parts [18], predicting the mechanical properties [12][19], and generating/validating component capability profiles as a tool to generate parts optimised design [20].

One of the most critical defects occurring in FDM is warpage, a geometric distortion typically observed on a flat and thin part. During the process, the filament extruded at the melting temperature cools due to the surrounding air in the printing chamber, resulting in a contraction that is prevented by the supporting platform. Both tensile and compressive stresses arise, and when the part is removed from the platform at the end of the process, these stresses are released causing a bending distortion [21]. Modelling strategies

have been proposed to estimate the effect of process parameters on the warpage of the part. The phenomenon is typically described utilizing the thermo-elasticity theory already developed for thermal stresses in structures assuming an elastic and isotropic material with a perfect bond between the layers. One-, two- or three- dimensional models have been developed [22-25], and the comparisons with both experimental results and finite element analysis [21], [26-30] have shown that the understanding of the influence of the variables associated to the part geometry, part material, and process on the warpage represent a challenging multi-objective optimization problem. Hence, the selection of a suitable polymeric material that would allow a prescribed warpage tolerance for a defined geometry is a significant challenge particularly at the initial stage where the exploration of the whole possible design space can lead to ineffective trial-and-error attempts to minimize the final warpage. A traditional modelling approach would result in either inaccurate - as the case for most of the analytical models – or time-consuming – as for most of the finite element analysis. A fast and accurate predicting tool is needed to obtain a reliable prediction of the resulting warpage for a defined material and geometry and to provide eventually indications to material scientists for developing a new class of polymers able to meet the manufacturing needs.

The scope of this work is to develop a versatile ML framework for FDM manufacturing applications in which part warpage can be predicted with respect to the selected material, part geometry, and process parameters. This will be accomplished considering the following sub-goals:

1. Estimation of the part warpage as a function of machine parameters, part geometry, and mechanical and thermal properties of common polymers used in FDM;
2. Classification of printable/non-printable parts based on a targeted level of warpage threshold;
3. Regression analysis to relate part geometry and chamber temperature in the space of the printable configurations based on the selected warpage threshold.

2 Methods

2.1 Overview

The part deflection due to warpage considered in this work is based on the analysis from Armillotta et al. [21]. Here the authors provided new hypotheses based on multiple-layer shrinkage and plastic deformation to justify the observed influence of part height on warpage. The new analytic formulation provides a better warpage prediction than the basic model obtained by Armillotta et al. and consistent with the assumptions of analytic models present in the literature [22]. Nonetheless, the improved model gives a poor fit for long and thick parts built with small layer thickness, leading the authors to the conclusion that the model will have to be revised considering additional physical mechanisms.

Hence, in this work, the basic model formulation is considered since it allows to describe the proposed methodology in a much simpler fashion and to obtain data samples with limited computational effort. Once a better predictive tool is available (either analytic or finite element-based), the same approach can

easily be adapted. A range of material commonly used in FDM was selected, namely ABS, PLA, PEEK, and Nylon (PA12).

ML is applied for both classification and regression purposes.

Classification is performed to identify the combination of parameters, such as part length, part height, and material glass-transition temperature, which ensure the part printability according to a user-defined warpage threshold. This, in turn, allows distinguishing between relevant and irrelevant areas of the design space. In other words, it indicates whether a selected material for a chosen part geometry can be manufactured without exceeding the selected part warpage.

Regression is used on these relevant design space areas to provide a capability profile based on the considered parameters. The capability profile can then be used to predict the part warpage and to quickly evaluate the effect of both material and process parameters. To this aim, the validated capability profile is used to ascertain the effect of the chamber temperature on the part warpage.

2.2 Data samples generation

The considered equation of the inter-layer warpage δ is [21]

$$\delta = \frac{3}{4}\alpha(T_G - T_C)\frac{L^2\Delta h}{h^2}\left(1 - \frac{\Delta h}{h}\right) \qquad (1)$$

in which α is the linear shrinkage coefficients, T_G is the material glass transition temperature, T_C is the chamber temperature, L is the length of the part, *Δh* is the thickness of every deposited layer, and h is the height of the part.

Based on equation (1), two parameters P_1 and P_2 are defined, as the linear shrinkage coefficients α and the difference (T_G –T_C), respectively. All the other parameters represent the user initial input and are hence fixed. Equation (1) can be rewritten as

$$\delta = \frac{3}{4}P_1P_2\frac{L^2\Delta h}{h^2}\left(1 - \frac{\Delta h}{h}\right) \qquad (2)$$

Typical values for α, T_G , and recommended T_C (if indicated) for the selected materials are reported in Table 1. The resulting range values for P1 and P2 are reported in Table 2.

Table 1 *Materials and properties overview [21][31-32].*			
Material	**α (K^{-1})**	**T_G [°C]**	**T_C [°C]**
ABS	$60*10^{-6}$	95	75
PLA	$68*10^{-6}$	62	25 #
PEEK	$98*10^{-6}$	143	120
PA12	$95*10^{-6}$	70	25 #

 # T_C value not suggested and hence room temperature is considered

Table 2

Range of P1 and P2 values.

Parameter	**Range**
P1 [%]	60 ÷98
P2 [°C]	20 ÷ 45

Different P1-P2 combinations were generated by sampling according to a Sobol sequence [33] the design space constituted by the range values for P1 and P2. A database consisting of one thousand (1,000) P1-P2 data point combinations were selected. The sampling was performed in MatLab using the code developed by Bessa et al. [34]. Parts warpage were then computed with equation (2).

2.3 Machine Learning for printable/non-printable part classification

Support Vector Machine (SVM) algorithms were developed in MatLab to create a map of printable/non-printable configurations based on P1-P2 combinations that satisfy the condition of part warpages below a user-defined threshold. Bayesian ML method called scalable variational Gaussian process (SVGP) was chosen as the most adequate for this classification application [35].

Different test cases were investigated performing the proposed methodology for different warpage thresholds, as reported in Table 3. The part length L, the printed layer thickness Δh, and the part height h were kept constant to 100 mm, 0.254 mm, and 1.5 mm, respectively.

Table 3 Test cases overview for classification.			
Length *L [mm]*	Layer thickness *Δh [mm]*	Part height *h [mm]*	Warpage threshold *δ [mm]*
100	0.254	1.5	1.5
			2
			2.5

2.4 Machine Learning for regression in the classified space design

Linear Regression, Support Vector Machine, and Gaussian Process were the model classes analysed for the prediction of the part warpage for the P1-P2 combinations that were classified as printable. The warpage threshold was randomly set to 2 mm. Firstly, the regression models were built via the MatLab "Regression Learner" application for the lowest part height (1.5 mm) and the best model was then applied to the other two-part heights, namely 3.5 and 5.5 mm, as shown in Table 4.

Cross-validation of 10 folds for the training data was used to protect from overfitting. The comparison of classification performance was performed in terms of the root mean squared error (RMSE) and the training time.

Table 4 Test cases overview for regression.			
Part Length *L [mm]*	Layer thickness *Δh [mm]*	Warpage threshold *δ [mm]*	Part height *h [mm]*
100	0.254	2	1.5
			3.5
			5.5

2.5 Validation and Application

The regression model was then validated against Equation 2 in terms of the resulting warpage values for different part heights. In Table 5 the considered variables for the regression model validation are reported.

Table 5

Parameters considered for the regression model validation.

Part Length *L [mm]*	Layer thickness *Δh [mm]*	Part height *h [mm]*	Chamber Temperature T_C [°C]
100	0.254	1.5-7.5	75

Lastly, the validated model was applied for evaluating the influence of the chamber temperature on the warpage of the part. More details are provided in the corresponding results section.

3 Results

3.1 Data samples generation

Figure 2 shows the P1-P2 data points obtained by sampling the defined design space. Based on these data points, the warpage values were computed via (2) and reported in Fig. 3.

3.2 Machine Learning for printable/non-printable part classification

According to the different warpage thresholds, the SVGP method provided the combination of P1-P2 that would ensure a part within the defined warpage limit, i.e. printable if the part warpage is below the threshold and not printable otherwise, as depicted below in Fig. 4 for the three considered warpage thresholds.

3.3 Machine Learning for regression in the classified space design

Table 6 shows the regression performances of the trained models for each class for the lowest part height (1.5 mm).

Table 6
Performances of the best model for each regression class; part height 1.5 mm.

Class	**Best type**	**RMSE**	**Training time [s]**
Linear Regression	Linear	$3.66*10^{-5}$	6.1
Support Vector Machine	Coarse	$1.85*10^{-5}$	3.7
Gaussian Process	Squared Exponential	$3.52*10^{-5}$	20

The best model both in terms of the RMSE and the training time values resulted to be the Coarse Support Vector Machine (CSVM). Figure 5 shows the true response vs. the predicted response, i.e. the warpages computed with Eq. 2 vs. the warpages predicted by the CSVM. A diagonal line is also plotted, representing a perfect match between analytic and predicted values. The vertical distance from the line to any point is the error of prediction for that point.

The CSVM model is then used to perform the regression for parts of 3.5 and 5.5 mm of height. The comparisons between the predicted and the analytic warpage values are reported in Figs. 6 and 7.

An improved prediction capability can be seen for the part heights of 3.5 and 5.5 mm due to a larger number of the dataset upon which the model is built. In fact, for the higher part heights, all the warpage values are below the selected threshold and hence more samples are considered. Table 7 present the comparison of the RMSE, training time, and the number of data points for the three addressed part heights. It is evident that for a larger number of data points the RMSE reduces up to one order of magnitude. Conversely, the effect of a larger dataset on the training time is negligible.

Table 7
Model performances for different layer heights; CSVM model, warpage threshold 2 mm.

Part height *h* [mm]	**Dataset**	**RMSE**	**Training time [s]**
1.5	663	$1.85*10^{-5}$	3.7
3.5	1000	$6.1*10^{-6}$	5.9
5.5	1000	$2.3*10^{-6}$	3.1

3.4 Validation and Application

Figure 8 shows the comparison between the CSVM and the analytic models. A good agreement is obtained between the two models, especially for part height below 4.5 mm (difference $\leq$ 0.01 mm).

The developed CSVM model can now provide the information of what range of chamber temperature T_C can be selected to obtain a warpage value below a desired threshold for the selected part geometry, layer

thickness, number of printed plies, and the selected material. The final selection of the material implies the definition of both the shrinkage coefficient, i.e. P1, and of the T_G. Hence, P1 is fixed and P2 can differ among all the P2 values that have been related to printable parts. The T_C can then be computed from the selected P2 values, along with the resulted part warpage.

For the described application, the considered material, geometry of the part, and warpage threshold are reported in Table 8. Five (5) P2 values (i.e. 5 T_C values since T_G is fixed for a given material) were selected among the P2 values belonging to the data points classified as printable. Figure 9 shows the part warpage variation concerning different chamber temperatures obtained with both the analytic model and the CSVM regression.

Table 8
Parameters selected for the CSVM application.

Material	Warpage threshold δ [mm]	Part height h [mm]	Part Length L [mm]	Layer thickness Δh [mm]	Chamber Temperature range T_C [°C]
ABS	2	1.5	100	0.254	25–75

4 Discussion

The proposed methodology represents an ML-based approach for the evaluation of the influence of material, geometry, and process parameters on the resulting warpage in FDM parts.

The flexibility and the efficiency provided by ML is very promising to take into account the effect of different combinations of part geometry and manufacturing parameters so that a first-time-right manufacturing process can be developed.

The availability of numerous data points is essential for proper ML algorithm training. The warpage values were obtained by Eq. (2) which has the great advantage of providing as many as needed data points in a very short time, without the burden of conducting experimental tests. The main drawback is however represented by the accuracy of the analytic model itself. Other work, such as [Armillotta], showed the inaccuracy of Eq. (2). Other approaches must be used to ensure a better predictive tool, for examples based on finite element models. Most importantly, the analytic equation can be easily used to perform the presented work without a clear need for ML. Nonetheless, most of the manufacturing process cannot be easily described by formulas, especially if the influence of several different parameters is the object of investigation, and therefore the analytic approach is here used only to demonstrate the feasibility of the methodology.

The SVM algorithm used to classify the parts as printable or not printable is based on two design parameters P1 and P2, which take into account the material shrinkage coefficient, the glass-transition

temperature, and the printer chamber temperature. Results, as expected, show a larger number of P1-P2 combinations for printable parts for higher values of warpage threshold.

Regression is performed within the data points classified as printable. A model based on CSVM is deployed so that the warpage value for a specific combination of P1 and P2 parameters is predicted. The comparison between the analytic and the predicted data show very good accuracy of the model, especially for higher part heights of 3.5 and 5.5 mm.

ABS is then considered to validate the CSVM model and to show how the proposed approach can be used to relate the part warpage to the temperature of the printing chamber. As expected, the warpage increases for lower chamber temperatures in a very good agreement with the analytic prediction.

Further research can be based on this methodology especially for taking into account more complex process parameters and part geometry to tailor the manufacturing process for a selected material and a desired part property value/limit. In addition, if experimental data are available, this ML-based approach has the significant advantage of discard the need for the understanding of all the complex phenomena that have to be provided in any reliable analytic or numerical predictive model. This represents a powerful tool that can highly support the generations of future optimised 3D printed components.

5 Conclusion

The scope of this work is to present a versatile framework for the adoption of ML as a supporting agent in FDM manufacturing. The work is based on the definition of a material type and a part geometrical configuration and to apply ML for (i) part classification as printable/non-printable based on the selected part material and geometry with respect to the desired warpage threshold, (ii) prediction of the part warpage below the selected threshold as a function of the chamber temperature.

The methodology has also the significant advantage of providing both quick end reliable prediction of the influence of manufacturing process parameters on a prescribed manufacturing outcome, e.g. the part warpage. In this context, the approach is adaptable to different materials, part geometry, manufacturing process parameters, and interested manufacturing output.

This work can be recognized as a concrete demonstration of the effectiveness of ML for FDM and manufacturing processes in general. Lastly, not only quick predictions can be made directly from the available experimental or modelling data, but also, and more notably, indications on which material/part geometry combination provides the best-desired outcome can lead to new solutions virtually achieving a first-time-right manufacturing process.

Declarations

Funding

Not applicable.

Conflicts of interests

The author declares that he has no conflict of interests.

Availability of data and material

Not applicable

Code availability

The MatLab codes used in this work will be provided by the author upon request

References

1. Solomon IJ, Sevvel P, Gunasekaran J, “A review on the various processing parameters in FDM”, Materials Today: Proceedings, 37, 509–514, 2021
2. Popescu D, Zapciu A, Amza C, Baciu F, Marinescu R (2018) FDM process parameters influence over the mechanical properties of polymer specimens: a review. Polymers Testing 69:157–166
3. Sood AK, Ohdar RK, Mahapatra SS (2010) Parametric appraisal of mechanical property of fused deposition modelling processed parts. Materials Design 31:287–295
4. Mohamed OA, Masood SY, Bhowmik JL (2015) Optimization of fused deposition modeling process parameters: a review of current research and future prospects. Advanced Manufacturing 3:42–53
5. Anitha R, Arunachalam S, Radhakrishnan P (2001) Critical parameters influencing the quality of prototypes in fused deposition modelling. J Mater Process Technol 118:385–388
6. Dey A, Yodo N (2019) A systematic survey of FDM process parameter optimization and their influence on part characteristics. Journal of Manufacturing Materials Processing 3:64
7. Stavropoulos P, Foteinopoulous P (2018) Modelling of additive manufacuting process: a review and classification. Manuf Rev 5:1–26
8. Alafaghania A, Qattawi A, Alrawi B, Guzman A (2017) Experimental optimization of fused deposition modelling processing parameters: a design-for-manufacturing approach. Procedia Manufacturing 10:791–803
9. Mohan N, Senthil P, Vinodh S, Jayanth N (2017) A review on composite materials and process parameters optimisation for the fused deposition modelling process. Virtual Physical Prototyping 12:47–59
10. Onwubolu GC, Rayegani F, “Characterization and optimization of mechanical properties of ABS parts manufactured by the fused deposition modelling process”, International Journal of Manufacturing

Engineering, 2014, 1–13. 2014

11. Lanzottu A, Grasso M, Staiano G, Martorelli M (2015) The impact of process parameters on mechanical properties of parts fabricated in PLA with an open-source 3-D printer. Rapid Prototyping Journal 21(5):604–617
12. Garzon-Hernandez S, Garcia-Gonzalez D, Jerusalem A, Arias A (2020) Design of FDM 3D printed polymers: an experimental modelling methodology for the prediction of mechanical properties. Mater Des 188:1–10
13. Chacon JM, Caminero MA, Garcia-Plaza E, Nunez PJ (2017) Additive manufacturing of PLA structures using fused deposition modelling: effect of process parameters on mechanical properties and their optimal selection. Mater Des 124:143–157
14. Croccolo D, De Agostinis M, Olmi G (2013) Experimental characterization and analytical modelling of the mechanical behaviour of fused deposition processed parts made of ABS-M30. Comput Mater Sci 79:506–558
15. Zhu Z, Anwer N, Huang Q, Mathieu L (2018) Machine learning in tolerancing for additive manufacturing. CIRP Annals – Manufacturing Technology 67:157–160
16. Jin Z, Zhang Z, Ott J, Gu GX (2021) Precise localization and semantic segmentation detection of printing conditions in fused filament fabrication technologies using machine learning. Additive Manufacturing 37:101696
17. Hooda N, Chohan JS, Gupta R, Kumar R, “Deposition angle prediction of Fused Deposition Modeling process using ensemble machine learning”, ISA Transactions, 2021, article in press
18. Charalampous P, Kostavelis I, Kontodina T, Tzovaras D (2020) Learning-based error modelling in FDM 3D printing process. Rapid Prototyping Journal. DOI 10.1108/RPJ-03-2020-0046
19. Zhang J, Wang P, Gao RX (2019) Deep learning-based tensile strength prediction in fused deposition modeling. Comput Ind 107:11–21
20. Goudswaard M, Hicks B, Nassehi A (2020) The creation of a neural network based capability profile to enable generative design and the manufacture of functional FDM parts. The International Journal of Advanced Manufacturing Technologies 113:2951–2968
21. Armillotta A, Bellotti M, Cavallaro M (2018) Warpage of FDM parts: Experimental tests and analytic model. Robotics Computer-Integrated Manufacturing 50:140–152
22. Wang TM, Xi JT, Jin Y (2007) A model research for prototype warp deformation in the FDM process. The International Journal of Advanced Manufacturing Technologies 33:1087–1096
23. Xinhua L, Shengpeng L, Zhou L, Xianhua Z, Xiaohu C, Zhongbin W (2015) An investigation on distortion of PLA thin-plate part in the FDM process. The International Journal of Advanced Manufacturing Technologies 79:1117–1126
24. Zhang Y, Chou YK, “Three-dimensional finite element analysis simulations of the Fused Deposition Modeling process”, Proc. IMechE Part B J. Eng. Manuf., 220, 1663–1671, 2006

25. Huang Q (2016) An Analytical Foundation for Optimal Compensation of Three-Dimensional Shape Deformation in Additive Manufacturing. J Manuf Sci Eng 138:1–8
26. Kuo CC, Wu YR, Li MH, Wu HW (2019) Minimizing warpage of ABS prototypes built with low-cost fused deposition modelling machine using developed closed-chamber and optimal process parameters. The International Journal of Advanced Manufacturing Technologies 101:593–602
27. Fitzharris ER, Watanabe N, Rosen DW, Shofner ML (2018) Effects of material properties on warpage in fused deposition modelling parts. The International Journal of Advanced Manufacturing Technologies 95:2059–2070
28. Cattenone A, Morganti S, Alaimo G, Auricchio F (2019) Finite Element Analysis of Additive Manufacturing Based on Fused Deposition Modeling: Distortions Prediction and Comparison With Experimental Data. J Manuf Sci Eng 141:1–17
29. Panda BN, Shankhwar K, Garg A, Jian Z (2017) Performance evaluation of warping characteristic of fused deposition modelling process. The International Journal of Advanced Manufacturing Technologies 88:1799–1811
30. Dilberoglu UM, Simsek S, Yaman U (2019) Shrinkage compensation approach proposed for ABS material in FDM process. Mater Manuf Processes 34:993–998
31. https://www.simplify3d.com/support/materials-guide/properties-table/
32. https://www.victrex.com/~/media/datasheets/victrex_tds_450g.pdf
33. Sobol IM (1976) Uniformly distributed sequences with an additional property of uniformity. Zh Vychisl Mat Mat Fiz 16(5):1332–1337
34. Bessa MA, Bostanabad R, Liu Z, Hu A, Apley DW, Brinson C, Chen W, Liu WK (2017) A framework for data-driven analysis of materials under uncertainty: Countering the curse of dimensionality. Comput Methods Appl Mech Eng 320:633–667
35. Bessa MA, Glowacki P, Houlder M (2019) Bayesian Machine Learning in Metamaterial Design: Fragile Becomes Supercompressible. Advanced Materials – Supporting Information 31:1904845

Figures

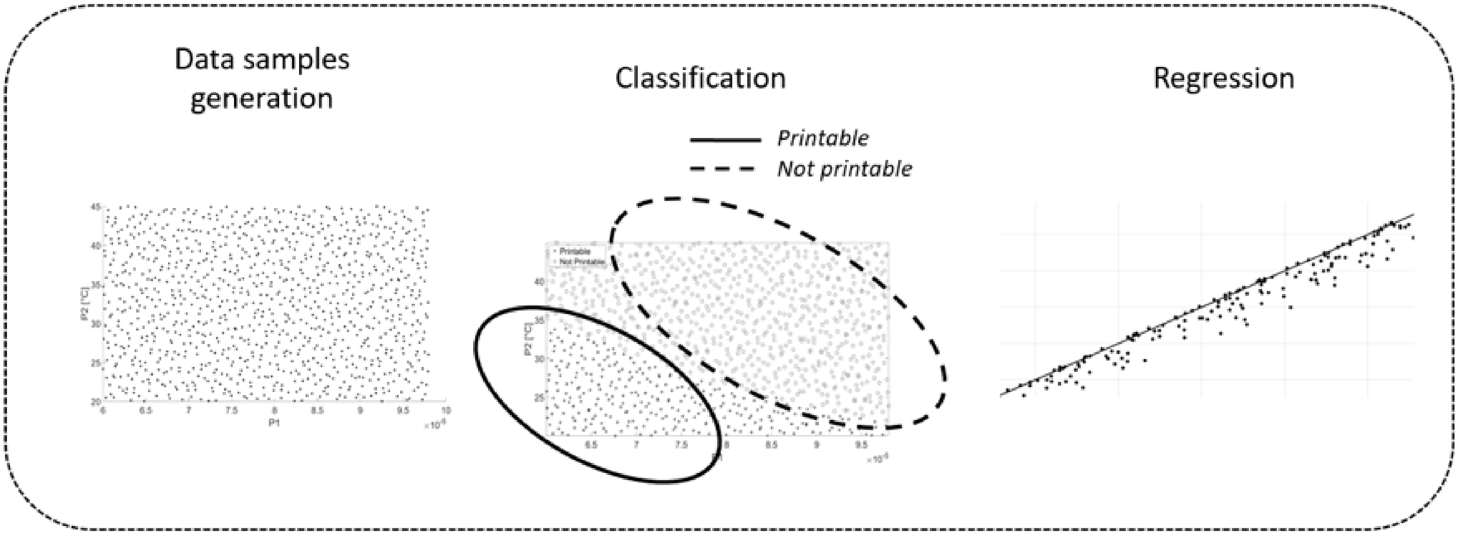

Figure 1

Approach overview.

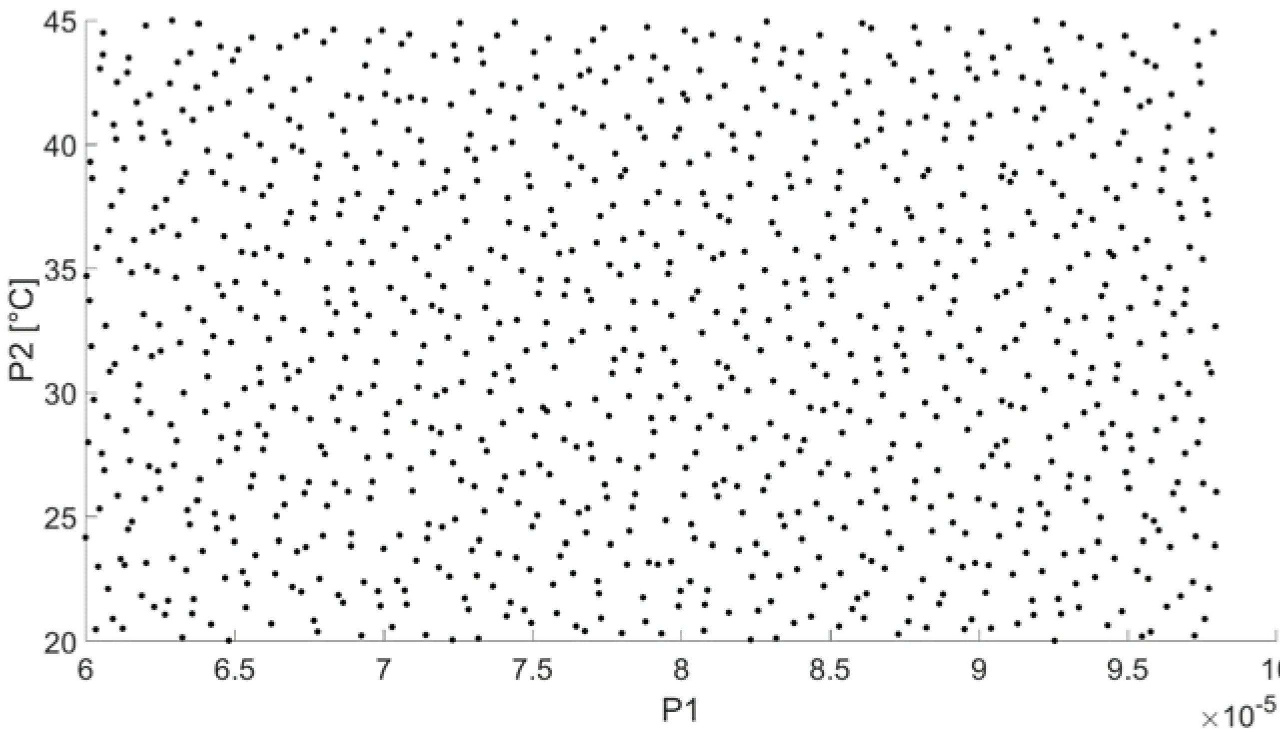

Figure 2

Combination of P1-P2 values in the sampled design space.

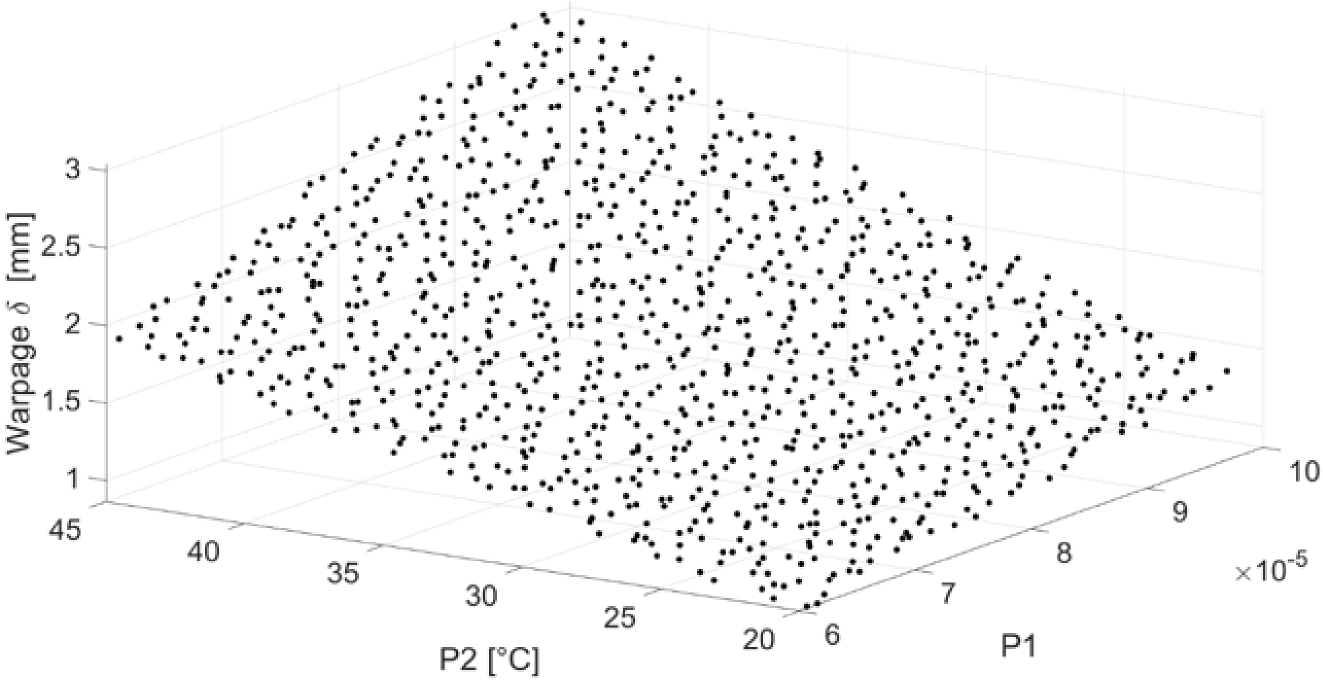

Figure 3

Warpage values based on the sampled P1-P2 data points.

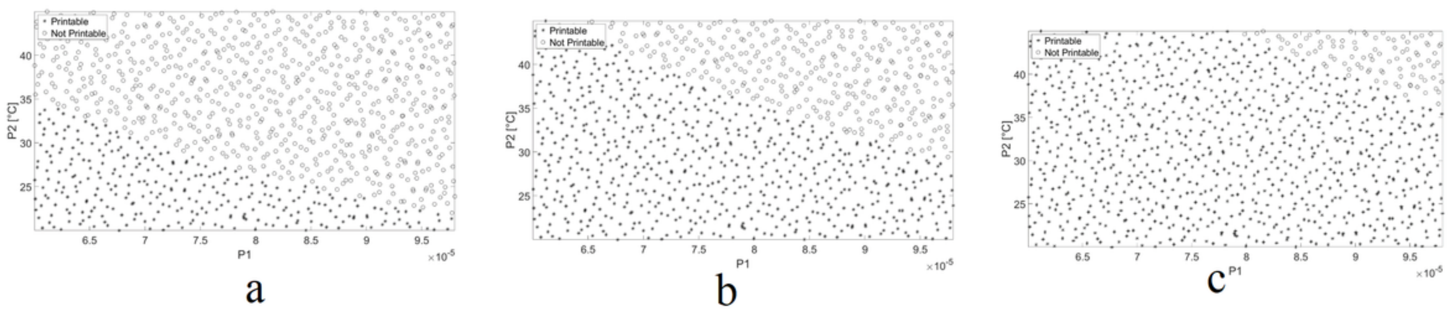

Figure 4

P1-P2 data points resulting in printable/not printable parts according to the selected warpage threshold: (a) 1.5 mm, (b) 2 mm, and (c) 2.5 mm.

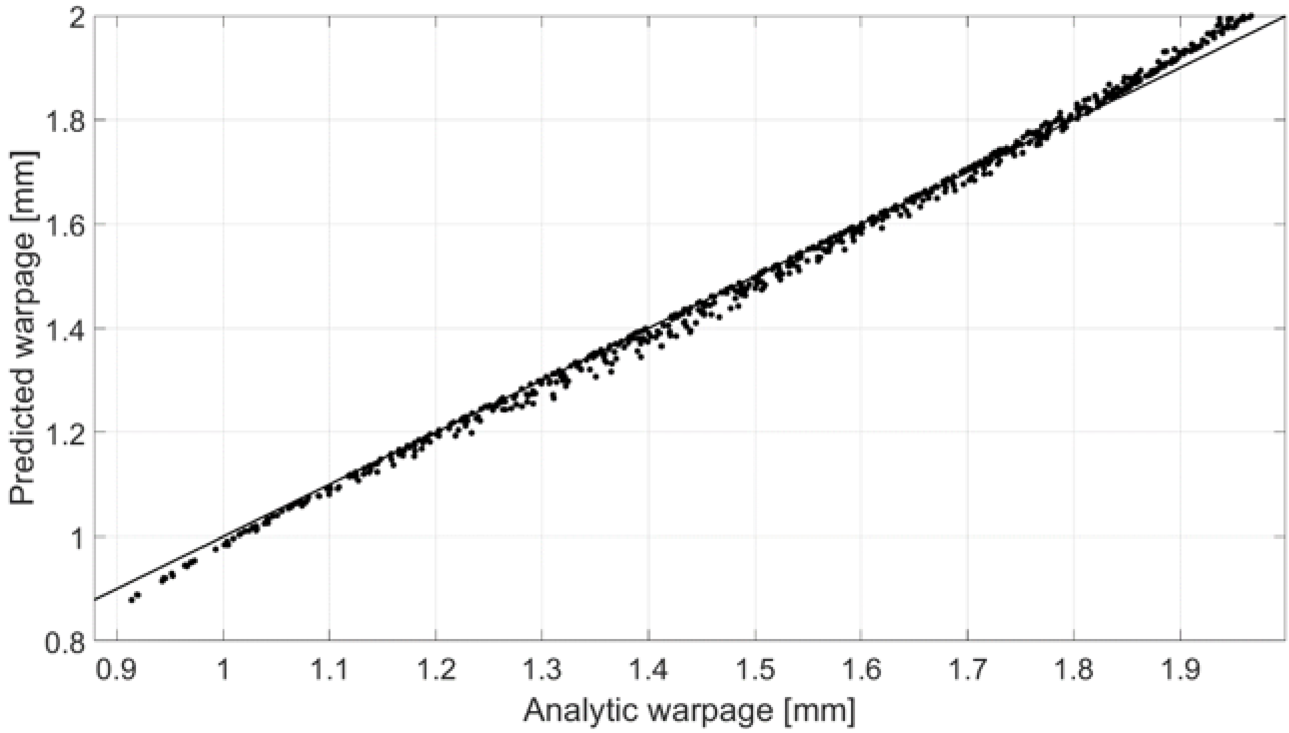

Figure 5

Analytic vs. predicted warpage for a 1.5 mm part height.

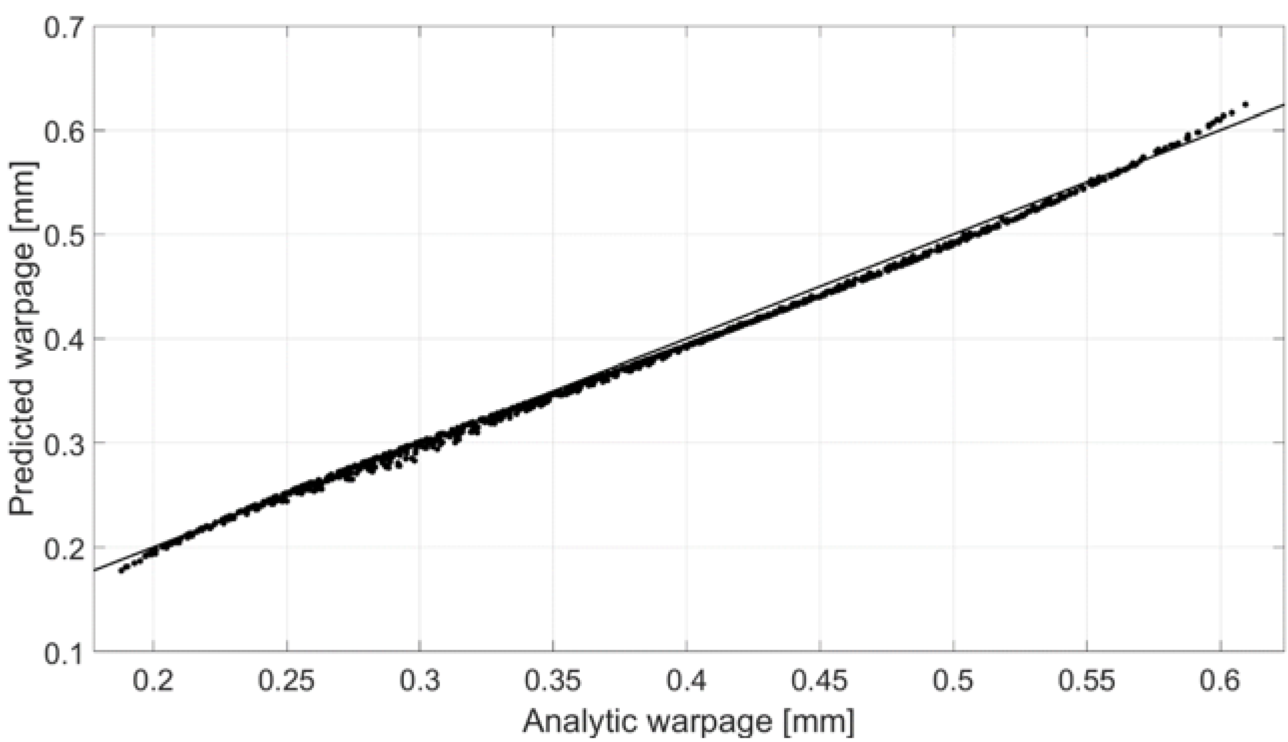

Figure 6

Analytic vs. predicted warpage for a 3.5 mm part height.

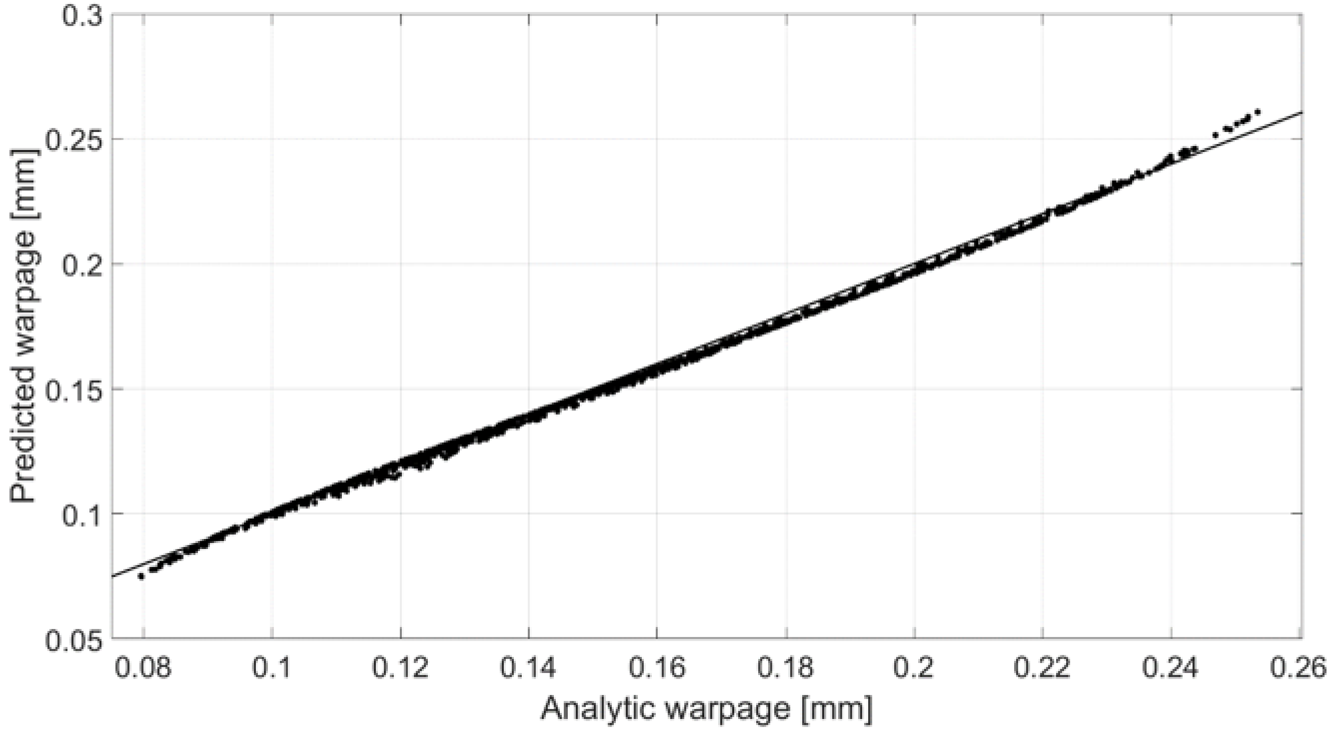

Figure 7

Analytic vs. predicted warpage for a 5.5 mm part height.

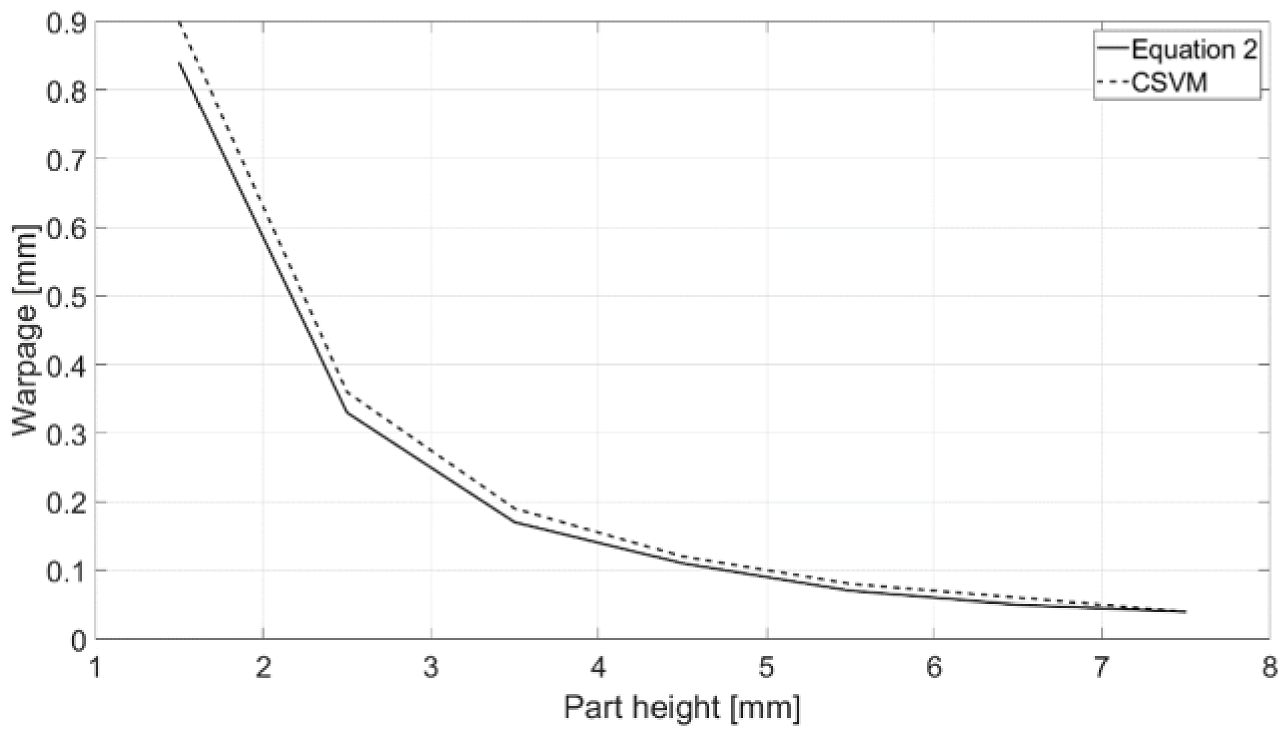

Figure 8

Comparison between the analytic model from equation 2 and CSVM regression model for different part heights for ABS material, part length 100 mm, layer thickness 0.254 mm, and TC 75° C.

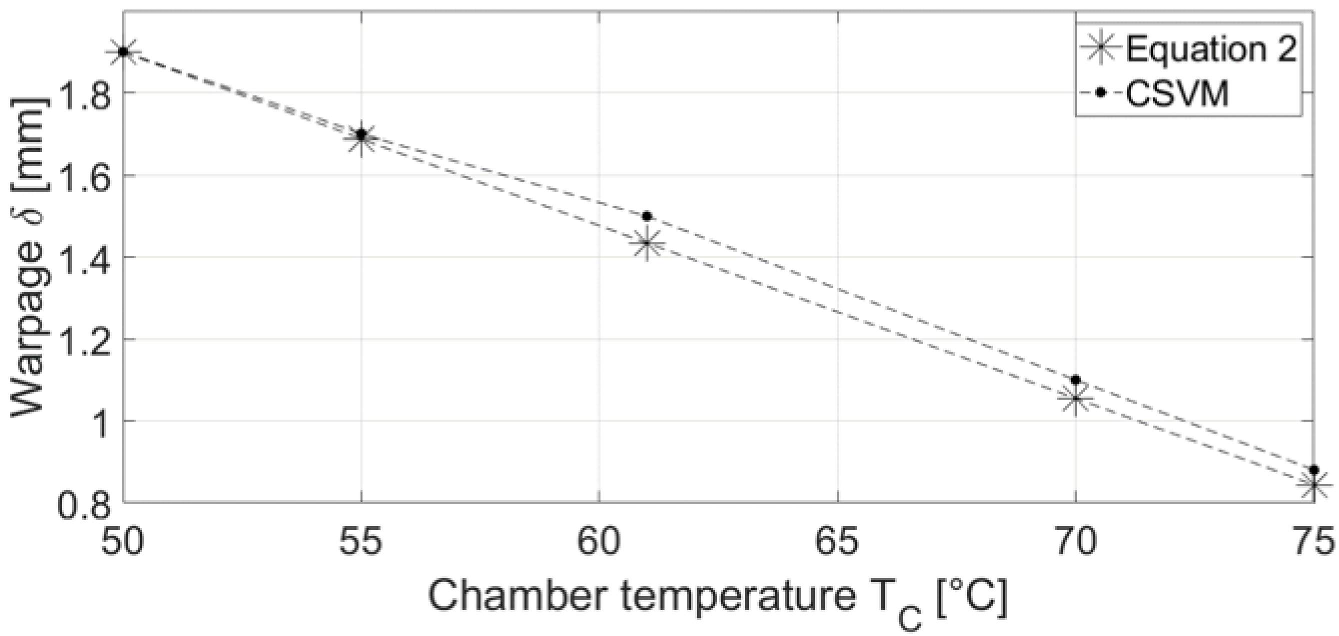

Figure 9

Warpage variation as a function of the chamber temperature.